J|A|C|S COMMUNICATIONS

Published on Web 12/10/2010

Formation of SnO_2 Hollow Nanospheres inside Mesoporous Silica Nanoreactors

Shujiang Ding,[†,§] Jun Song Chen,[†,§] Genggeng Qi,[‡] Xiaonan Duan,[‡] Zhiyu Wang,[†] Emmanuel P. Giannelis,[‡] Lynden A. Archer,*[,‡] and Xiong Wen Lou*[,†]

School of Chemical and Biomedical Engineering, Nanyang Technological University, 70 Nanyang Drive, Singapore 637457, and Kaust-Cornell Center for Energy and Sustainability, Cornell University, Ithaca, New York 14853, United States

Received September 28, 2010; E-mail: xwlou@ntu.edu.sg; laa25@cornell.edu

Abstract: We report an interesting approach for efficient synthesis of SnO_2 hollow spheres inside mesoporous silica "nanoreactors". The as-prepared products are shown to have a uniform size distribution and good structural stability. When evaluated for their lithium storage properties, these SnO_2 hollow spheres manifest improved capacity retention.

Hollow structures are of great interest due to their characteristics such as low density, high surface-to-volume ratio, and low coefficients of thermal expansion and refractive index compared to their solid counterparts. These outstanding properties render them promising for a spectrum of applications including lithium-ion batteries,[1−5] catalysis support,[6,7] drug/gene delivery,[8−10] and medical imaging/diagnostics.[11,12]

Procedures for synthesizing hollow nanospheres can be broadly divided into two categories: template-free and templating approaches. Even though template-free techniques generally involve fewer synthetic steps and are thus considered quite facile,[2,13] templating methods offer important advantages, including narrow-size-distribution products with well-defined structural features.[14,15] There are nevertheless inherent drawbacks in the template removal process, which limit the utility of the approach. Specifically, if the template core is removed by calcination at high temperature (e.g., to remove carbon or polystyrene spheres), or removed by chemical dissolution (e.g., use of hydrofluoric acid to remove silica templates), collapse of some fraction of the hollow structures is a virtual certainty. It is therefore highly desirable to develop new strategies for synthesizing hollow nanospheres that build on the strengths of both the templating and template-free methods.

In this communication, we report an interesting approach to synthesize metal oxide hollow nanospheres inside mesoporous silica (SiO_2) nanoreactors. We use molten metal salt hydrate (a highly concentrated salt solution with a melting temperature below 100 °C) as a precursor, which is able to diffuse into the hollow cavity of the SiO_2 nanoreactors via the mesoporous shell. The excess amount of precursor outside the nanoreactors can be easily washed away thus ensuring exclusive loading of precursor inside the nanoreactors. After controlled thermal annealing, the metal salt is transformed into its corresponding metal oxide *in situ* and, thereby, forms a shell on the inner surface of nanoreactors, giving rise to a double-shelled metal oxide@SiO_2 hollow structure. The outer SiO_2 shell is then easily removed by HF etching to obtain metal oxide hollow spheres (*caution: HF is highly corrosive and must be handled with great care!*). In this approach, the SiO_2 mesoporous nanoreactor plays crucial roles by confining and supporting the metal oxide during the thermal treatment. As a result, the metal oxide hollow nanospheres are formed with both uniform size distribution and good structural integrity. The size of as-formed hollow spheres can also be readily tuned by changing the dimensions of the nanoreactor cavity. Here, we choose SnO_2 as an example to simultaneously demonstrate the concept and to prepare hollow nanospheres relevant for applications as an anode material in lithium-ion batteries (LIBs). Compared with SnO_2 solid particles and spheres, the as-prepared SnO_2 hollow nanospheres manifest improved lithium storage properties.

Scheme 1 illustrates the procedure for generating SnO_2 hollow spheres. We first soak the SiO_2 nanoreactors into molten

Scheme 1. Schematic Formation of SnO_2 Hollow Spheres inside Mesoporous Silica Nanoreactors

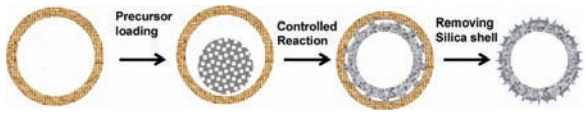

$SnCl_2 \cdot 2H_2O$ (T_m = ~37 °C), which can easily diffuse into the hollow cavity through the mesoporous channels. The excessive precursor remained outside the nanoreactors is removed by rinsing with ethanol and then water. After washing, the SiO_2 nanoreactors with precursor loaded are heated at 700 °C in air to obtain SnO_2@SiO_2 double-shelled hollow spheres. Due to this special conformation, the subsequent removal of the outer mesoporous SiO_2 shell by HF etching is more facile than dissolving solid SiO_2 cores,[1,3,5] and the inner SnO_2 shell is left intact, granting much better structural stability compared to conventional templating approaches.

We first examine the morphology of the SiO_2 mesoporous hollow spheres with field-emission scanning electron microscopy (FESEM) and transmission electron microscopy (TEM). From the FESEM image (Figure 1A), it can be clearly observed that the SiO_2 nanoreactors are very uniform with a relatively smooth surface and a diameter of about 400 nm. The TEM image (Figure 1A, inset) shows that the shell has a thickness of about 30 nm. These mesoporous nanoreactors have a very high surface area of 1300 $m^2\ g^{-1}$ and an average pore size of 3.08 nm,[16] which is large enough to provide an easy access to the internal void space.[17] The morphology of SnO_2@silica double shells is shown in Figure 1B, and it can be clearly seen that the dark SnO_2 shell, which is about 50 nm in thickness, is attached on the inner surface of SiO_2 nanoreactors. After removing SiO_2 with a HF solution, the SnO_2 hollow spheres are obtained with a relatively rough surface (Figure

[†] Nanyang Technological University.
[‡] Cornell University.
[§] These authors contributed equally.

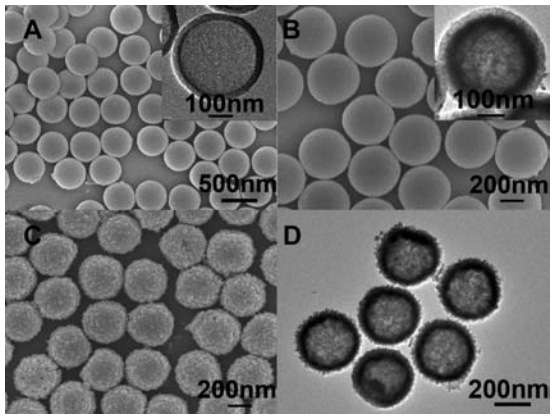

Figure 1. (A) SEM and TEM (inset) images of mesoporous silica hollow spheres with a diameter of 400 nm; (B) SEM and TEM (inset) images of SnO_2@silica double shells; (C, D) SEM and TEM images of SnO_2 hollow spheres, which are prepared by removing silica with 2 wt % HF solution for 30 min.

1C and D). The outer diameter is about 340 nm, which is consistent with the cavity size of SiO_2 nanoreactors (Figure 1A). The energy-dispersive X-ray analysis (EDX; see Supporting Information, Figure S1) shows that the residual SiO_2 is lower than 0.5 wt %, and the atomic ratio of Sn and O elements is about 0.5, which indicates that the hollow spheres are mostly composed of SnO_2.

By employing SiO_2 nanoreactors with different cavity sizes, we are able to produce SnO_2 hollow nanospheres with a smaller diameter using the same approach (see Supporting Information, Figure S2), highlighting the versatility of our method.

In order to further understand the formation mechanism, we carry out some experiment to investigate the effect of annealing temperature. After annealing at a relatively low temperature of 120 °C, the precursor (probably a partially hydrolyzed form) appears almost amorphous and exists as a sphere inside each nanoreactor because the melting point of these metal salt hydrates is also quite low (see Supporting Information, Figure S3). Crystalline SnO_2 starts to form when annealed at 200 °C and becomes dominant only after annealing at 300 °C. It is thus suggested that the SnO_2 shell formation, from decomposition/oxidation of hydrates, is a result of a strong interaction between metal oxide and SiO_2 surface. This might be partly verified by the observation of the hairy surface of the resulting SnO_2 hollow nanospheres (Figure 1C and D). It is also found that a high annealing temperature of 700 °C is required to obtain structurally robust SnO_2 hollow spheres that can sustain the removal of silica nanoreactors.

The crystal structure of the SnO_2 hollow spheres is determined by X-ray diffraction (XRD), as shown in Figure 2. All the identified

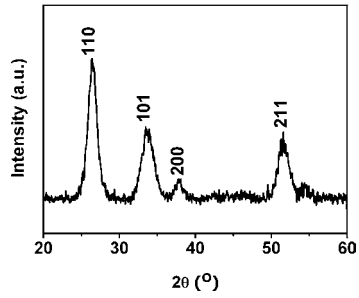

Figure 2. XRD pattern of SnO_2 hollow spheres.

peaks can be assigned to tetragonal SnO_2 (JCPDS card no. 41-1445, SG: $P4_2/mnm$, $a_o = 4.738$ Å, $c_o = 3.187$ Å).[2] The mesoporous structure of the SnO_2 hollow spheres is confirmed by the N_2 adsorption/desorption isotherm (see Supporting Information, Figure S4), illustrating a type-IV isotherm with a type-H3 hysteresis loop.[18] The narrow pore size distribution (Figure S4, inset) calculated using the Barrett−Joyner−Halenda (BJH) method from both the adsorption and desorption branches of the isotherm indicates that most of the pores have a diameter in the range of 2−5 nm. Such a porous structure leads to a Brunauer−Emmett−Teller (BET) specific surface area of 46 $m^2\ g^{-1}$.

As an n-type wide-band gap ($E_g = 3.6$ eV) semiconductor, SnO_2 is one of the most widely investigated materials owing to its important technological applications such as gas sensors[19] and lithium-ion batteries (LIBs).[2] When SnO_2 serves as the active material in a lithium-ion battery, the reaction mechanism can be described as follows: $SnO_2 + 4Li^+ + 4e^- \rightarrow Sn + 2Li_2O$ (1); $Sn + xLi^+ + xe^- \leftrightarrow Li_xSn$ ($0 \le x \le 4.4$) (2).[2,20] SnO_2-based anode materials have attracted much attention due to their theoretical reversible capacity of 790 mA h g^{-1}, which is more than twice that of the currently used graphite (370 mA h g^{-1}).[20] However, the practical use of these anode materials is significantly impeded by the poor capacity retention over long-term charge−discharge cycling. This problem mainly originates from the large volume change of electrode materials accompanying Li insertion and extraction (reaction (2); the volume change is more than 200% when Sn alloys with Li to form $Li_{4.4}Sn$), which creates large internal stress, leading to the disintegration of the electrode material, and eventually destroys conduction pathways between neighboring particles.[20] To relieve this problem, one effective strategy is to design hollow and/or porous nanostructures, where the concept is to utilize the local empty space, i.e., the pores or the hollow interior, to partially buffer the large volume change,[2,20,21] thus improving the cyclic capacity retention of the electrode material upon extended cycling.

To reveal the advantage of the hollow structure, we compared the lithium storage properties of the as-prepared SnO_2 hollow nanospheres with those of other solid counterparts, namely, SnO_2

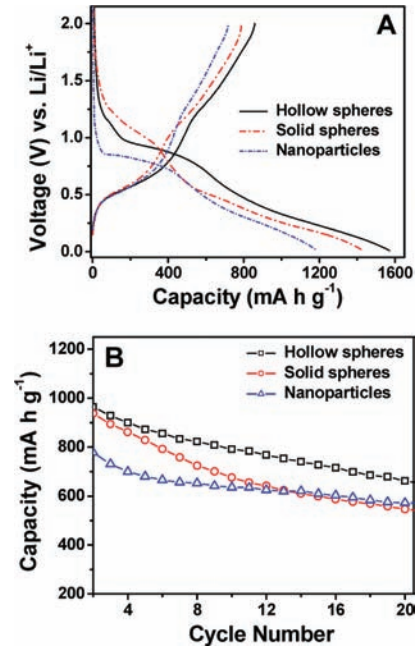

Figure 3. Comparative lithium storage properties of the as-prepared SnO_2 hollow nanospheres, SnO_2 solid spheres, and SnO_2 nanoparticles: (A) Charge−discharge profiles, and (B) Cycling performance. All of the measurements were conducted at a current rate of 160 mA g^{-1} with a voltage window of 0.01−2.0 V.

solid particles and spheres. Figure 3A shows the discharge−charge voltage profiles of the three samples at a constant current density of 160 mA g^{-1}. The voltage profiles are consistent with that of SnO_2-based anodes.[2,20] It is clear that the SnO_2 hollow nanospheres show the highest discharge capacity of 1571 mA h g^{-1} among the three samples. A possible reason for the hollow nanospheres having a higher lithium storage capacity is because of the internal void space, which probably helps to store more lithium.[2] While both spherical samples are able to deliver a subsequent charge capacity of ∼800 mA h g^{-1}, the nanoparticles sample can only have ∼700 mA h g^{-1}. This leads to a similar initial irreversible loss in the three samples, which is about 40%. This is quite common to SnO_2-based electrode materials,[2] and such a large initial irreversible loss is attributed to the irreversible reduction of SnO_2 to Sn as described by eq 1 and other possible irreversible processes, such as the formation of solid electrolyte interface (SEI).

The lithium insertion/extraction process in the SnO_2 hollow nanospheres is further characterized with cyclic voltametry (CV). The CV behavior (see Supporting Information, Figure S5) is generally consistent with previous reports,[2] indicating a similar electrochemical pathway. The characteristic pair of current peaks is observed at potentials (cathodic/anodic) of 0.05/0.73 V in the first cycle. This is attributed to the alloying (cathodic sweep) and dealloying (anodic sweep) processes that are highly reversible and mainly responsible for the reversible lithium storage capacity. From the second cycle onward, a broad cathodic band (0.75−1.25 V) with a corresponding anodic band (1.25−1.9 V) appears pronounced, possibly suggesting partial reversibility of reaction 1.

Figure 3B shows the comparative cycling performance of SnO_2 hollow spheres and the other two solid counterparts with a voltage window of 0.01−2 V at a current rate of 160 mA g^{-1}. It is apparent that the as-prepared SnO_2 hollow nanospheres demonstrate much better lithium storage properties compared to the other two samples, in terms of both storage capability and cyclic capacity retention. This is indeed in support of the above concept that the hollow interior will lead to improved lithium storage properties of SnO_2-based anodes. The postmortem study shows that the hollow structure is somewhat retained after 20 charge−discharge cycles (Figure S6). The cycling performance of the as-prepared SnO_2 hollow nanospheres up to 50 cycles is shown in Figure S5B. Despite the obvious advantage over the solid counterparts, the as-prepared SnO_2 hollow spheres do not show perfect performance. However, it has been demonstrated that the performance can be significantly improved by coating hollow SnO_2 spheres with a thin layer of carbon materials.[5]

In summary, we have demonstrated a novel and efficient top-down approach to synthesize SnO_2 hollow spheres inside mesoporous silica nanoreactors. The as-prepared SnO_2 hollow spheres are shown to have a uniform size distribution, good structural stability, and enhanced lithium storage properties. The current strategy for making hollow spheres is new, considering that no conventional template is introduced in the system and the method is quite different from the common one-pot template-free techniques. A perhaps obvious appeal of our approach is that it might be extended to generate other metal oxide hollow nanospheres, such as CuO and Fe_xO_y.

Acknowledgment. The authors are grateful to the Ministry of Education (Singapore) for financial support through the AcRF Tier-1 funding (RG 63/08, M52120096) and to King Abdullah University of Science and Technology (KAUST) for supporting this work under Award No. KUS-C1-018-02.

Supporting Information Available: Detailed experimental procedures, more TEM and SEM images, EDX results, N_2 adsorption−desorption isotherm, XRD patterns, and cyclic voltammograms. This material is available free of charge via the Internet at http://pubs.acs.org.

References

(1) Lou, X. W.; Archer, L. A.; Yang, Z. C. *Adv. Mater.* **2008**, *20*, 3987.
(2) Lou, X. W.; Wang, Y.; Yuan, C. L.; Lee, J. Y.; Archer, L. A. *Adv. Mater.* **2006**, *18*, 2325.
(3) Lou, X. W.; Yuan, C.; Archer, L. A. *Small* **2007**, *3*, 261.
(4) Yin, X. M.; Li, C. C.; Zhang, M.; Hao, Q. Y.; Liu, S.; Chen, L. B.; Wang, T. H. *J. Phys. Chem. C* **2010**, *114*, 8084.
(5) Lou, X. W.; Li, C. M.; Archer, L. A. *Adv. Mater.* **2009**, *21*, 2536.
(6) Liang, H. P.; Zhang, H. M.; Hu, J. S.; Guo, Y. G.; Wan, L. J.; Bai, C. L. *Angew. Chem., Int. Ed.* **2004**, *43*, 1540.
(7) Arnal, P. M.; Comotti, M.; Schuth, F. *Angew. Chem., Int. Ed.* **2006**, *45*, 8224.
(8) Chen, J. F.; Ding, H. M.; Wang, J. X.; Shao, L. *Biomaterials* **2004**, *25*, 723.
(9) Zhu, Y. F.; Shi, J. L.; Shen, W. H.; Dong, X. P.; Feng, J. W.; Ruan, M. L.; Li, Y. S. *Angew. Chem., Int. Ed.* **2005**, *44*, 5083.
(10) Liu, J.; Qiao, S. Z.; Hartono, S. B.; Lu, G. Q. *Angew. Chem., Int. Ed.* **2010**, *49*, 4981.
(11) Chen, J.; Saeki, F.; Wiley, B. J.; Cang, H.; Cobb, M. J.; Li, Z. Y.; Au, L.; Zhang, H.; Kimmey, M. B.; Li, X. D.; Xia, Y. *Nano Lett.* **2005**, *5*, 473.
(12) Hirsch, L. R.; Stafford, R. J.; Bankson, J. A.; Sershen, S. R.; Rivera, B.; Price, R. E.; Hazle, J. D.; Halas, N. J.; West, J. L. *Proc. Natl. Acad. Sci. U.S.A.* **2003**, *100*, 13549.
(13) Li, J.; Zeng, H. C. *Angew. Chem., Int. Ed.* **2005**, *44*, 4342.
(14) Yang, Z. Z.; Niu, Z. W.; Lu, Y. F.; Hu, Z. B.; Han, C. C. *Angew. Chem., Int. Ed.* **2003**, *42*, 1943.
(15) Caruso, F.; Caruso, R. A.; Mohwald, H. *Science* **1998**, *282*, 1111.
(16) Qi, G. G.; Wang, Y. B.; Estevez, L.; Switzer, A. K.; Duan, X. N.; Yang, X. F.; Giannelis, E. P. *Chem. Mater.* **2010**, *22*, 2693.
(17) (a) Deng, Y. H.; Cai, Y.; Sun, Z. K.; Liu, J.; Liu, C.; Wei, J.; Li, W.; Liu, C.; Wang, Y.; Zhao, D. Y. *J. Am. Chem. Soc.* **2010**, *132*, 8466. (b) Qi, G. G.; Wang, Y.; Estevez, L., Duan, X. N.; AnakoN. Park, A. A.; Li, W.; Jones, C. W.; Giannelis, E. P. *Energy Environ. Sci.* **2011**, DOI:10.1039/c0ee00213e.
(18) Kruk, M.; Jaroniec, M. *Chem. Mater.* **2001**, *13*, 3169.
(19) Kuang, Q.; Lao, C. S.; Wang, Z. L.; Xie, Z. X.; Zheng, L. S. *J. Am. Chem. Soc.* **2007**, *129*, 6070.
(20) Chen, J. S.; Li, C. M.; Zhou, W. W.; Yan, Q. Y.; Archer, L. A.; Lou, X. W. *Nanoscale* **2009**, *1*, 280.
(21) Han, S. J.; Jang, B. C.; Kim, T.; Oh, S. M.; Hyeon, T. *Adv. Funct. Mater.* **2005**, *15*, 1845.

JA108720W